Histone H1 compacts DNA under force and during chromatin assembly

Botao Xiao[a,b,*], Benjamin S. Freedman[c,*], Kelly E. Miller[c], Rebecca Heald[c], and John F. Marko[a,d]
[a]Department of Physics and Astronomy and [d]Department of Molecular Biosciences, Northwestern University, Evanston, IL 60208; [b]Department of Biological Chemistry and Molecular Pharmacology, Harvard Medical School, and Boston Children's Hospital, Boston, MA 02115; [c]Molecular and Cell Biology Department, University of California, Berkeley, Berkeley, CA 94720

ABSTRACT **Histone H1 binds to linker DNA between nucleosomes, but the dynamics and biological ramifications of this interaction remain poorly understood. We performed single-molecule experiments using magnetic tweezers to determine the effects of H1 on naked DNA in buffer or during chromatin assembly in *Xenopus* egg extracts. In buffer, nanomolar concentrations of H1 induce bending and looping of naked DNA at stretching forces below 0.6 pN, effects that can be reversed with 2.7-pN force or in 200 mM monovalent salt concentrations. Consecutive tens-of-nanometer bending events suggest that H1 binds to naked DNA in buffer at high stoichiometries. In egg extracts, single DNA molecules assemble into nucleosomes and undergo rapid compaction. Histone H1 at endogenous physiological concentrations increases the DNA compaction rate during chromatin assembly under 2-pN force and decreases it during disassembly under 5-pN force. In egg cytoplasm, histone H1 protects sperm nuclei undergoing genome-wide decondensation and chromatin assembly from becoming abnormally stretched or fragmented due to astral microtubule pulling forces. These results reveal functional ramifications of H1 binding to DNA at the single-molecule level and suggest an important physiological role for H1 in compacting DNA under force and during chromatin assembly.**

Monitoring Editor
Kerry S. Bloom
University of North Carolina

Received: Jul 13, 2012
Revised: Oct 17, 2012
Accepted: Oct 19, 2012

INTRODUCTION

The dynamics and functional ramifications of linker histone H1 binding to DNA remain poorly understood. Histone H1 is a positively charged, stoichiometric component of nucleosome arrays possessing a short amino terminus, a central winged-helix DNA-binding motif, and a long, unstructured carboxy terminus (Ramakrishnan *et al.*, 1993). H1 is larger and more soluble at lower salt concentrations than core histones and is dispensable for the assembly or maintenance of beads-on-a-string nucleosome arrays (Happel and Doenecke, 2009). Evidence that H1 compacts chromatin comes primarily from in vitro experiments using purified and reconstituted chromatin templates, where H1 protects the linker DNA between nucleosomes from nuclease digestion and promotes compaction of nucleosome arrays into 30-nm chromatin fibers (Thoma *et al.*, 1979; Weischet *et al.*, 1979). Cryo–electron microscopy and hydroxyl-radical footprinting suggest that the different domains of H1 interact with multiple DNA-binding sites, and a specific H1-mediated stem structure within linker DNA has been observed, supporting the hypothesis that H1 functions by binding both incoming and outgoing strands of linker DNA and neutralizing the negative charge of the phosphate backbone (van Holde and Zlatanova, 1996; Syed *et al.*, 2010), although direct crystallographic evidence for this mechanism is lacking. In vivo, H1 is difficult to deplete, and hence its functional significance remains poorly characterized, but its presence has been correlated with increased interphase nucleosome repeat length and compaction of interphase chromatin and mitotic chromosomes in some systems (Fan *et al.*, 2005; Freedman and Heald, 2010).

In addition to its function on nucleosome arrays, H1 also has the ability to bind and noncovalently cross-link DNA in vitro in the

This article was published online ahead of print in MBoC in Press (http://www.molbiolcell.org/cgi/doi/10.1091/mbc.E12-07-0518) on October 24, 2012.

*These should be considered as joint first authors.

Address correspondence to: Botao Xiao (botao.xiao@childrens.harvard.edu; botaoshaw@hotmail.com).

Abbreviations used: dH1, H1-depleted; dMock, mock-depleted; NASP, nuclear autoantigenic sperm protein.

Supplemental Material can be found at:
http://www.molbiolcell.org/content/suppl/2012/10/22/mbc.E12-07-0518v1.DC1.html

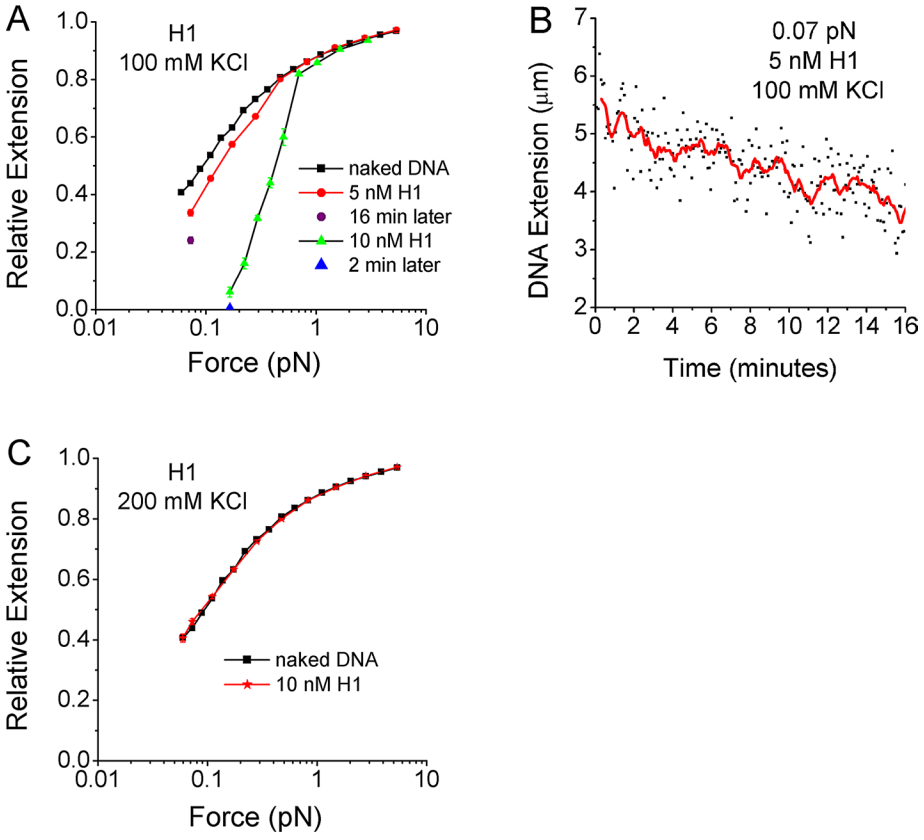

FIGURE 1: Dependence of DNA condensation on force, H1, and salt conditions. (A) DNA extension measured as the force decreased in 100 mM KCl (XB buffer). In 5 nM H1 solution, the DNA extensions for forces of >0.6 pN were the same as in the buffer (naked DNA). The extension decreased as the holding force was reduced step by step from 0.6 to 0.07 pN. Each step lasted about 2 min, during which the extensions were measured. In separate samples, 10 nM H1 was added, and the DNA extension was measured as the force decreased from 5 to 0.2 pN. Between 0.2 and 1 pN, the DNA compaction ratios in 10 nM H1 were higher than in 5 nM H1. Each experimental data point, presented as the mean value, was obtained from 15 measurements. (B) DNA extension decreased with time in 5 nM H1 solution with a holding force of 0.07 pN. The extension decreased from 5.6 to 3.7 μm in 16 min (A, 16 min later) and to ~0.1 μm in 1 h. (C) In contrast to A, no compaction was observed for 10 nM H1 in 200 mM KCl buffer (XB + KCl) with a holding force of >0.1 pN.

complete absence of nucleosomes. For example, H1 has been observed to bind to a 420–base pair plasmid fragment with a dissociation constant (K_D) of 18 nM. If the same DNA formed a dinucleosome template, the K_D decreased to 7.4 nM (Ura *et al.*, 1996), suggesting stabilization of H1 binding by interactions with nucleosomes (Kaplan *et al.*, 2009). Much like core histones (Thastrom *et al.*, 2004), H1 has been observed to bind DNA tightly, with a strong dependence on salt concentration. NaCl and $MgCl_2$ strongly modulate H1–DNA interactions (Clark and Thomas, 1986; Al-Natour and Hassan, 2007): noncooperative binding occurs for concentrations of <20 mM, cooperative binding occurs at >50 mM, and dissolution of H1–DNA complexes occurs at >400 mM. In the cooperative mode, complexes between H1 and linear DNA may appear as either aggregates or linear "tramlines" consisting of two side-by-side DNA duplexes joined by H1 "ties" (Clark and Thomas, 1986; Thomas *et al.*, 1992). This interaction between histone H1 and naked DNA has not been characterized in detail, and its relation to chromatin structure in vivo is unclear.

Fluorescence recovery after photobleaching experiments reveal H1 to be highly dynamic in vivo, with residence times on chromatin of only seconds (Brown, 2003; Freedman and Heald, 2010). In buffer, H1 binds to sperm nuclei at ~30-fold higher stoichiometry than is typically found in vivo and displays much longer residence times, whereas addition of cytoplasm to this reaction reduces H1 binding and restores its rapid dynamics (Freedman *et al.*, 2010). These results raise the question of how H1–DNA function differs in vitro versus in vivo on the single-molecule level. Previous single-molecule studies with individual chromatin fibers show that linker histones stabilize the folding of these fibers; they do not affect chromatin stiffness or torsional plasticity (Kruithof *et al.*, 2009; Recouvreux *et al.*, 2011). Notably, the effect of H1 on naked DNA was not investigated in these studies, and the nucleosomes were assembled from minimal components in buffer rather than in complex cytoplasm. We therefore sought to measure the effect of histone H1 on the force dynamics of single DNA molecules in buffer or cytoplasm and investigate the possibility of additional roles for histone H1 on chromatin and DNA.

RESULTS

H1 compacts naked DNA under force

We first determined the range of force within which H1 can affect single linear DNA. Single λ–DNA tethers (48.5 kb, 16.5 μm in length) were assembled and verified as single-molecule tethers by measurement of their force–extension response in phosphate-buffered saline (PBS; ~150 mM univalent salt), which was then replaced by a *Xenopus*-extract-compatible XB buffer, which contains 100 mM KCl. No difference among force–extension relations was observed in PBS versus XB buffers. The DNA tether was held with a 5-pN force, which stopped DNA compaction. After different concentrations of H1 solutions were introduced, the holding force was decreased stepwise from 5 to 0.07 pN. Each step lasted about 2 min, during which 28 data points were obtained measuring extension of the DNA by an autofocus method (Skoko *et al.*, 2004).

In 5 nM H1 solution, DNA extension did not change until the holding force decreased to 0.6 pN or less (Figure 1A; DNA extensions are given relative to naked DNA contour length). Below 0.6 pN, extension decreased and did not reach equilibrium during the 2-min duration of each fixed force; the extensions are averaged at each force point. The extensions decreased more rapidly as the force decreased. At the lowest force studied, 0.07 pN, the extension decreased from 5.6 to 3.7 μm in 16 min (Figure 1B). Because naked DNA was 7.5 μm long at 0.07 pN, the H1-driven compaction ratio was 51%.

When 10 nM H1 solution was used in the assay, single-DNA extensions progressed to zero (100% compaction) in only 2 min when force was reduced to 0.2 pN. At each force, the compaction ratios for 10 nM H1 were higher than for 5 nM H1 (Figure 1A). These data demonstrate that H1 is capable of compacting naked DNA in buffer in a dose-dependent manner and counteracting forces in the range of 0.2–0.6 pN.

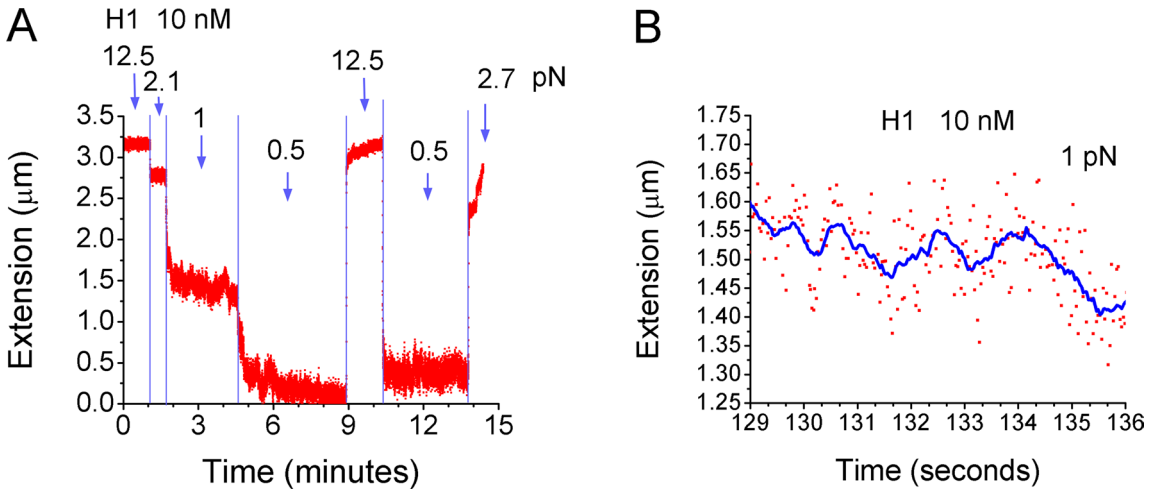

FIGURE 2: DNA bending and looping by H1. (A) The extension remained stable with 12.5- and 2.1-pN holding forces in 10 nM H1. The thermal fluctuations are ~150 nm around a fixed extension at 2.1 pN. After the force dropped to 1 pN, the extension decreased rapidly at the beginning and slowed down in ~4 min. The force was further decreased to 0.5 pN. The extension decreased to 0 in ~8 min. At 10 nM H1, a relatively low concentration, continuous nanometer-scale decreases are suggestive of compaction by bending. Larger, hundreds-of-nanometer drops strongly suggest loop formation. When force was subsequently increased to 12.5 pN the extension jumped to approximately the length of naked DNA. On switching from 12.5 to 0.5 pN, the extension dropped again. Finally, a force increase to 2.7 pN increased the DNA extension. (B) Expanded view of compaction at 1 pN described in A. The thermal fluctuations at 1 pN are ~200 nm. The DNA was observed to undergo compaction by 20- to 100-nm decreases (smoothed data). Results similar to those shown in A and B were observed in five separate experiments.

To test the effects of salt concentration, we introduced a solution containing 10 nM H1 in 200 mM KCl buffer into the flow cell. In contrast to 100 mM KCl, the 10 nM H1 plus 200 mM KCl DNA force–extension curve matched that of naked DNA in 200 mM KCl, that is, no compaction was observed (Figure 1C). These single-molecule results are consistent with previous studies showing reduced binding of H1 to DNA at increased salt concentrations (Clark and Thomas, 1986; Al-Natour and Hassan, 2007).

H1 bends and loops DNA

To observe the dynamic behavior of DNA compaction by H1, we measured extensions of supercoilable pRJ2421 DNA (9.5 kb) at a rate of ~34 times per second by a fast extension-measurement method (Skoko *et al.*, 2006). The extension remained stable with a 2.1-pN holding force in a solution containing 10 nM H1 in XB buffer. After the force was reduced to 1 pN, the extension proceeded to drop in increments ranging from ~20 to 500 nm (Figure 2, A and B). A 20-nm decrease at 1 pN (Figure 2B) corresponds to "loss" of a roughly 70–base pair DNA segment. The small ~20-nm decreases, along with the force–extension curves (Figure 1A), suggest that H1 can bend DNA. In contrast, our observation of hundreds-of-nanometer decreases suggests that H1 can also loop DNA, that is, cross-link it at two or more points. Reduction of force to 0.5 pN resulted in further DNA condensation to nearly zero length (Figure 2A).

Immediately after the DNA condensation, the holding force was increased to 12.5 pN. DNA extension jumped abruptly to approximately the length of naked DNA. On switching from 12.5 to 0.5 pN, the extension dropped sharply back down to <0.5 μm in 1 s. We note that this final extension is much less than the ~3-μm extension that would be expected of naked 9.5-kb DNA. A subsequent 2.7-pN force was also sufficient to increase the extension to a near-naked DNA value (Figure 2A).

DNA compaction in chromatin assembly reactions using *Xenopus* egg extracts

An interaction between histone H1 and naked DNA might be encountered in vivo early during the process of chromatin formation, before nucleosome assembly. We therefore investigated how H1 affects DNA undergoing chromatin formation in interphase *Xenopus* egg extract, which is devoid of endogenous DNA but contains stores of histones and other factors that rapidly assemble chromatin onto exogenous DNA. Endogenous H1 was first immunodepleted by >95% using a specific anti-H1 antibody, resulting in an H1-depleted (dH1) extract. The antibody was specific for embryonic histone H1, also known as H1M/B4/H1foo, which is the only isoform of histone H1 present in *Xenopus* eggs and early development until the mid-blastula transition. H1 is translated during oogenesis and is already stockpiled as protein in the *Xenopus* egg, making RNA interference or morpholino-based approaches less suitable than immunodepletion (Smith *et al.*, 1988). Sperm nuclei incubated in dH1 extracts are remodeled into nuclei, and mitotic chromosomes lack embryonic H1 but contain other chromatin components in normal stoichiometries (Dasso *et al.*, 1994; Maresca *et al.*, 2005). A wild-type extract was mock depleted using the same depletion procedures as for dH1 but using nonspecific rabbit immunoglobulin G (IgG) instead of anti-H1 antibody and was therefore named IgG-depleted (dMock). dH1 extracts could be rescued by readdition of recombinant H1 (dH1+H1). Because H1 binds more weakly to chromatin in cytoplasm than in buffer, it was added to dH1 extracts at 1.5 μM, which approximates H1's physiological concentration (Freedman and Heald, 2010; Freedman *et al.*, 2010).

Recent atomic force microscopy studies indicate that DNA incubated in extracts diluted 1:2 with buffer forms saturated nucleosome arrays, whereas 1:20 diluted extracts generate a mixture of nucleosomes and free DNA (Fu *et al.*, 2011). To determine appropriate reaction conditions, we first tested the ability of extracts at various

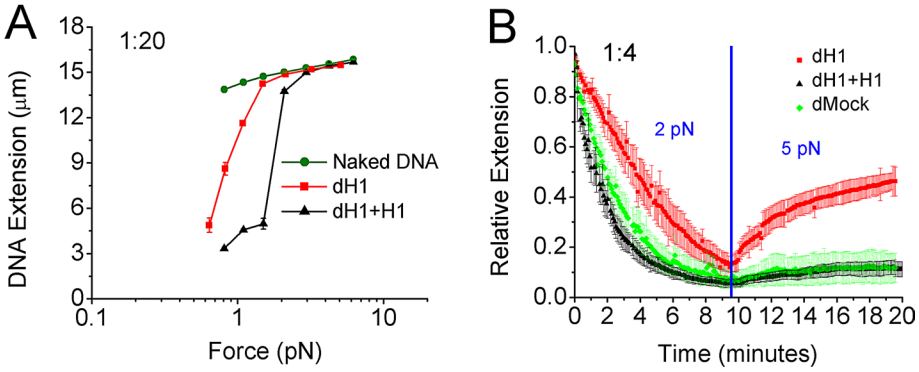

FIGURE 3: DNA compaction in dH1, dMock, and dH1+H1. A. Averages of DNA extension decreased as the holding force was reduced progressively from 5 to ~0.6 pN. The depleted extract (dH1, red square) and dH1 extract plus H1 (dH1+H1, black triangle) were both diluted 20 times (1:20). Each force step took 1 min. At each force, the compaction ratio for dH1 extract was smaller than for dH1+H1 extract. Each experimental data point, presented as the mean value, was obtained from ~15 measurements. (B) Smoothed time series of DNA compaction in dH1, dMock, and dH1+H1 extracts diluted four times (1:4). The force was initially held at 5 pN for 5 min and then reduced to 2 pN to allow chromatin assembly. The dH1 had slower assembly rates and longer end length than the dMock and dH1+H1. After 10 min, the force was increased to 5 pN. The extension of dH1 increased faster than for dMock and dH1+H1. Each data point is presented as an average and standard error obtained from three or four separate experiments.

dilutions to assemble chromatin, using micrococcal nuclease digestion and DNA supercoiling assays. All of the reaction conditions supported assembly of nucleosomes onto DNA over a period of several hours. One nucleosome per 160–180 base pairs was found on DNA plasmids by gel analyses (Supplemental Figure S1A). Efficient supercoiling of naked DNA was observed in 20-fold–diluted extracts, and even 100-fold–diluted extracts were capable of supercoiling at a somewhat reduced rate (Supplemental Figure S1B). These results are in agreement with previous chromatin assembly experiments in *Xenopus* egg extracts (Bennink *et al.*, 2001; Pope *et al.*, 2005).

To investigate H1 function across a spectrum of chromatin and naked DNA templates, we diluted dMock, dH1, and dH1+H1 extracts 1:4 or 1:20 in XB buffer and applied them to tethered DNA under force. The force on the bead was raised to 5 pN to keep DNA compaction from occurring when the *Xenopus* extract was introduced and held for an additional 5 min to allow the sample to reach equilibrium. For 1:20 extract with ATP, the DNA extensions were measured as the holding force was decreased stepwise from 5 to ~0.6 pN at 1-min intervals (Figure 3A). At each force, the compaction ratio for dH1 extract was smaller than for the dH1+H1 extract.

For 1:4 diluted extract in which DNA compaction occurs more rapidly, force was initially held at 5 pN for 5 min, during which no change in extension was observed, and subsequently reduced to 2 pN to allow chromatin assembly at controllable rates suitable for measurements. Time series were recorded during chromatin assembly (Figure 3B). After 5 min of assembly, the averaged relative extensions dropped to 37 ± 1% in dH1, longer than in dMock (18 ± 0.4%) and dH1+H1 (13 ± 0.1%; $p < 0.0001$). After 10 min, the final extension for dH1 (16 ± 1%) was longer than for dMock (7 ± 0.2%) and dH1+H1 (6 ± 0.1%; $p < 0.002$).

Similar experiments with 1:20 diluted extract at 0.7 pN were performed. After 60 min of assembly, the average relative extension of dH1 was 40 ± 1%, longer than for dMock (34 ± 1%) and dH1+H1 (29 ± 4%; $p < 0.05$; Supplemental Figure S2). Compared to the 1:4 dilution, the 1:20 dilution required a lower holding force and longer condensation time to reach the same relative extensions.

It was apparent that addition of H1 to the dH1 extract (dH1+H1) accelerates DNA compaction. Immediately after the assembly, the force was increased to 5 pN. After an additional 10 min of pulling, the extension of the chromatin formed in dH1 extract increased gradually to 46% of the original length. In contrast, the dH1+H1 increased to only 11% of the original length (Figure 3B); the dH1+H1 chromatin was more resistant to force-driven disassembly than were the dH1 fibers. We note that in single-chromatin-fiber experiments a force of 2 pN was initially applied to the fiber during assembly, which may limit the degree to which nucleosomes can be packed together. Taken together, these results suggest that compaction of the fiber upon reduction of the force to <2 pN, during which the effects of histone H1 were readily detectable, corresponds to the early stages of extract-mediated chromatin assembly.

H1 compacts sperm nuclei undergoing physiological chromatin assembly

Because the preceding work suggested a role for H1 in compacting naked DNA that has not yet been packaged into nucleosomes, we hypothesized that histone H1 might be important during the physiological remodeling of sperm nuclei into chromatin shortly after fertilization. During this process, sperm protamines are rapidly removed from the genomic DNA by cytoplasmic chaperones, resulting in decondensation. Although core histones bind to the DNA immediately, the assembly of mature nucleosomes requires topoisomerase activity and at least 30 min of time to assemble fully supercoiled DNA (Ruberti and Worcel, 1986). We therefore examined the role of H1 during this sensitive period of chromatin remodeling and assembly.

When sperm nuclei were added to dH1 extracts, a majority appeared abnormally elongated lengthwise (stretched) after 10 min compared with nuclei in wild-type extracts. This stretched appearance was retained even after nuclear envelope assembly at 30 min, but was not observed in dH1+H1 cytoplasm that had been reconstituted with recombinant H1 before the addition of the nuclei (Figure 4A). To quantify the extent of stretching, we measured the length of nuclei from the tail proximal to the aster to the distal tip. On average, nuclei were ~30% longer in dH1 extracts than in dMock and dH1+H1 (Figure 4B). In addition to stretching, a small proportion of nuclei in dH1 reactions appeared fragmented, showing loose, disconnected chromatin fibers after 10 min instead of an intact nucleus (Figure 4C). These fragmented nuclei accounted for approximately 8% of the structures in dH1 reactions, an enrichment of nearly 10-fold over dMock and dH1+H1 populations (Figure 4D).

Stretched and fragmented nuclei may have resulted from stretching and spreading forces generated by the associated microtubule aster, which assembled from the sperm centrosome during the first 10 min of the reaction (Figure 4, A and C). To test this hypothesis, we assembled nuclei in dH1 or dMock extracts supplemented with nocodazole, in which astral microtubule polymerization is suppressed. Consistent with our hypothesis, both the stretching and fragmentation phenotypes were greatly reduced in nocodazole-treated dH1

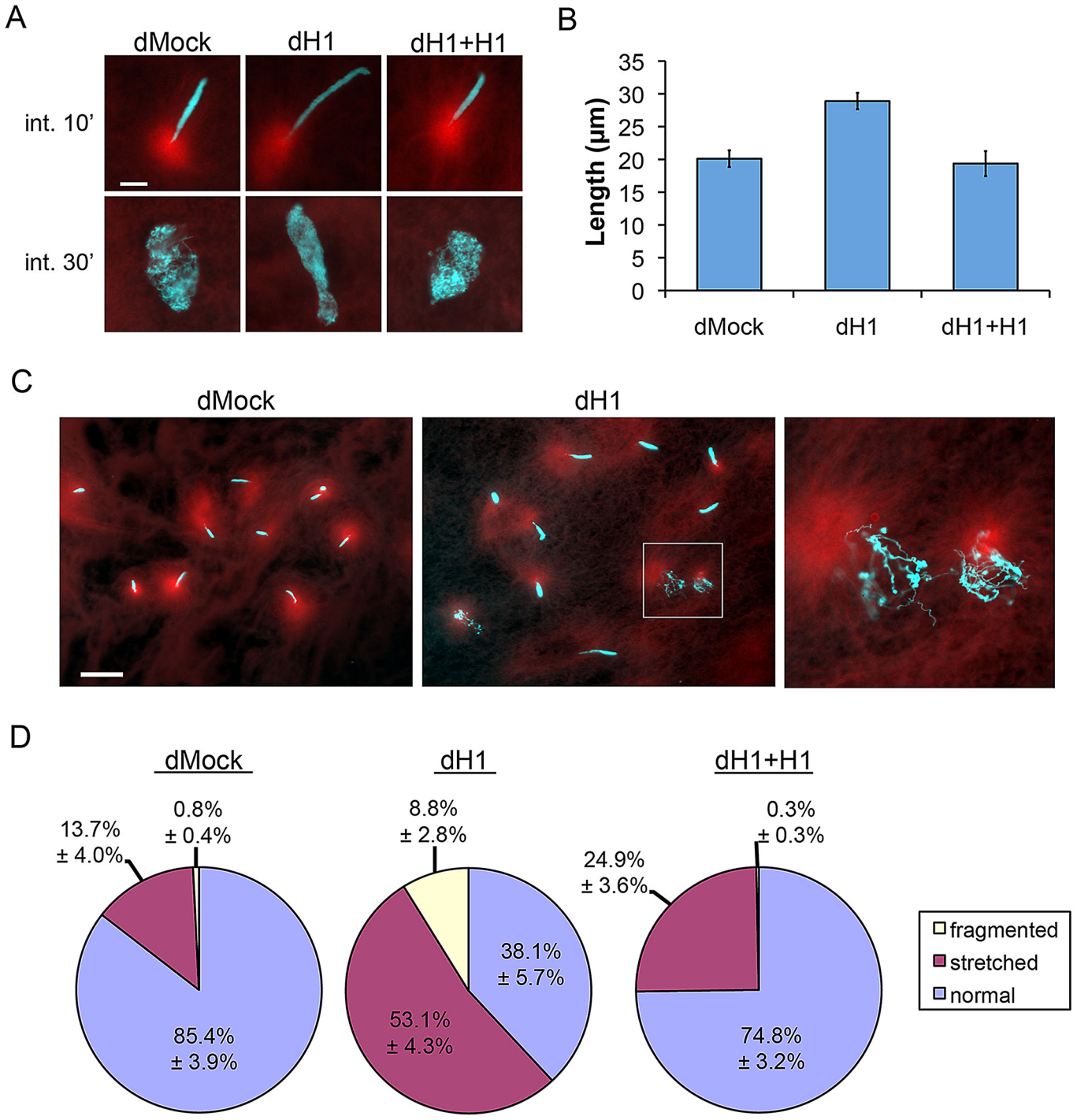

FIGURE 4: H1 stabilizes DNA during sperm nuclear remodeling. (A) Squash-fixed samples of IgG-depleted (dMock), H1-depleted (dH1), or H1-reconstituted (dH1+H1) egg extract reactions 10 and 30 min after the addition of sperm nuclei to interphase (int.) extracts. Red, rhodamine-labeled tubulin; aquamarine, DNA. Scale bar, 10 µm. (B) Measurement of sperm nuclear lengths from tail to tip in extract 10 min after addition of sperm nuclei. Mean sperm lengths were determined in separate experiments (~25 nuclei per experiment, $n \geq 3$ experiments per condition) and averaged. Error bars, SE. (C) Squash-fixed samples at 10 min showing multiple fragmented nuclei in the dH1 reaction. A close-up of the boxed region is shown at right. Scale bar, 50 µm. (D) Quantification of normal, stretched, and fragmented nuclei as a percentage of the total population 10 min after sperm addition (±SE; >250 nuclei were counted per condition).

extracts, which resembled nocodazole-treated dMock extracts (Supplemental Figure S3A). In the presence of nocodazole, the tail-to-tip length of nuclei was only slightly increased in dH1 reactions compared with dMock (Supplemental Figure S3B). Nuclear fragmentation was also reduced to background levels in the presence of nocodazole (Supplemental Figure S3C). These results support an

important role for histone H1 in stabilizing genomic DNA from astral pulling forces during physiological chromatin assembly and postfertilization nuclear remodeling, as predicted by our force–extension measurements.

DISCUSSION

Working with purified H1 excludes other intervening factors in chromatin and allows direct measurement of the H1–DNA interaction, which has not previously been examined at the single-molecule scale. Although present in only nanomolar concentrations, histone H1 is still present in excess relative to the single molecule of DNA in our experimental system and is therefore capable of compacting DNA extension by 51% at low holding forces (Figure 1A). The consecutive ≥20-nm (~70 base pairs and more) bending events at 1 pN in H1 solution (Figure 2B) are much smaller than 180 base pairs, the length of the DNA segment for a nucleosome. Taken together, these data suggest that the DNA in our single-molecule experiment has many binding sites for H1, and many of these are occupied at once. This is consistent with our recent observation that H1 is capable of binding to decondensed sperm chromatin in solution at ~30-fold–higher stoichiometry than it does in vivo (Freedman *et al.*, 2010).

Our fast-extension measurements recorded both bending and looping of DNA by H1 (Figure 2A). Looping may reflect the cross-linking of DNA strands (Skoko *et al.*, 2005) previously observed by atomic force microscopy (Clark and Thomas, 1986; Thomas *et al.*, 1992). It remains to be determined whether this cross-linking is mediated by a single molecule of H1 containing multiple DNA binding sites or by dimerization of two separate H1 molecules at different locations along the DNA strand.

To appreciate the effects of H1 on DNA, it is illuminating to compare it with *Escherichia coli* DNA-organizing proteins such as histone-like protein from *E. coli* strain U93 (HU) and factor for inversion stimulation (Fis), which we previously studied using similar methods (Xiao *et al.*, 2010, 2011; Graham *et al.*, 2011). At low protein concentrations of 5–20 nM, the compaction ratios from high to low are H1 > Fis > HU. On the other hand, the DNA binding constants obtained from previous studies are 400 nM to 29 μM for HU, 7.4–18 nM for H1, and tens to 0.2 nM for Fis. A reasonable explanation for these compaction ratios is that H1 appears capable of binding and cross-linking DNA at multiple sites into very compact structures, a function that might have evolved specifically for the protection and minimization of large eukaryotic genomes. In contrast, Fis and HU fold DNA into nucleoids in a prokaryotic cell, which lacks a distinct nucleus-like organelle.

In addition to its effects at nanomolar concentrations in buffer, H1 at a physiological concentration of 1.5 μM promotes increased compaction of DNA molecules under force undergoing chromatin assembly in egg extracts, resulting in faster apparent chromatin assembly rates and shorter chromatin extensions (Figure 3). This may reflect an additive effect of H1 and cytoplasmic chromatin assembly factors to the chromatin compaction process. Histone H1 may also affect chromatin assembly indirectly, for instance, by promoting closely folded or looped DNA topographies, which might facilitate the activity of core histones or topoisomerases. In buffer with nanomolar H1 concentrations, forces as low as 2.7 pN pull the DNA extension to that of naked DNA. In single-chromatin-assembly experiments in extracts, 5-pN force disassembles chromatin in dH1 extract more rapidly than in dH1+H1 extract, demonstrating again that H1 promotes chromatin assembly or stabilizes it. Meanwhile, even the more compact chromatin formed in dH1+H1 extract can be pulled open slowly, which indicates that the packaging is not irreversible.

Previous single-molecule studies of histone H1 did not observe compaction of chromatin (Kruithof *et al.*, 2009; Recouvreux *et al.*, 2011). In contrast, our experiments here reveal that depletion of histone H1 causes a significant increase in DNA and chromatin extension under force relative to chromatin assembled in dMock and dH1+H1 extracts and compacts decondensing sperm nuclei in egg cytoplasm (Figure 3). One explanation for this discrepancy is that previous measurements were performed on mature nucleosome arrays, whereas our experiments were performed on naked DNA or chromatin in the early stages of assembly. The effect of histone H1 may be easier to detect on these templates than on saturated nucleosome arrays, which are already maximally compacted. A second explanation is that chromatin assembled in our egg-extract-based experiments is close in structure to chromatin found in vivo and is consequently a better substrate for binding and compaction by H1 relative to chromatin-like fibers assembled from highly purified histones and DNAs carrying arrays of strong nucleosome-positioning sequences (Kruithof *et al.*, 2009; Recouvreux *et al.*, 2011).

Because the experimental system described here requires immunodepletion to remove endogenous histone H1, it is worth considering whether the phenotypes we observe could be influenced by codepletion of histone chaperones that interact with H1, such as NASP (Richardson *et al.*, 2000). The effect of codepletion can be functionally tested by comparing dMock, dH1, and H1-reconstituted (dH1+H1) extracts. Because the addition of bacterially expressed, recombinant histone H1 at the endogenous concentration is sufficient to rescue dH1 phenotypes (Figures 3 and 4 and Supplemental Figure S2), it is unlikely that these phenotypes are primarily due to codepletion of chaperones because these have not been replaced in the dH1+H1 condition. These experiments, together with the data from single-molecule experiments in buffer and cytoplasm (Figures 1–3), support a direct role for histone H1 in aggregating naked DNA and promoting DNA compaction. Minor differences between dMock and dH1+H1 conditions may be due to slight deficiencies in the concentration or conformation of recombinant H1 or its ability to fully complex with cytoplasmic chaperones compared with the endogenous protein. Chaperone proteins are likely to play an important role in facilitating and fine tuning H1–DNA interactions, a process that would be interesting to investigate in this system.

Given that core histone octamers can compact DNA to a greater extent than histone H1 alone, what advantage might histone H1 convey? Core histones compact DNA by physically wrapping it around a nucleosome octamer, a process that requires energy and time to organize and that in vivo is facilitated by topoisomerases. In contrast, the process by which histone H1 compacts DNA primarily involves the neutralization of negative charges upon binding and aggregation of separate DNA strands, processes that may occur more stochastically and rapidly. In cells, DNA is surrounded by a complicated aqueous environment in cells containing reducing and oxidizing agents, nucleases, topoisomerases, recombinases, active remodeling complexes, and nickases. DNA also moves frequently during transcription and duplication and is subjected to mechanical wear. Our observation that H1 compacts and protects DNA under force and during chromatin assembly is consistent with its proposed role in other situations in which nucleosomes are disrupted or linker DNA is suddenly exposed to cytoplasm, such as mitotic chromosome condensation (Maresca *et al.*, 2005) and DNA double-stranded break repair (Rosidi *et al.*, 2008; Freedman *et al.*, 2010). Dynamic binding of H1 would thus provide stability and protection while remaining loose enough to allow strand movement,

repair, nucleosome sliding, and the eventual transition to more mature chromatin structures.

MATERIALS AND METHODS

H1 protein expression and purification

Recombinant H1 of *Xenopus laevis* was obtained as described (Maresca *et al.*, 2005; Freedman and Heald, 2010; Freedman *et al.*, 2010). Briefly, the coding sequence of *X. laevis* embryonic H1 (also called H1M or B4) was cloned into vector pET30 with an NH_2-terminal hexahistidine (6His) tag. The tagged H1 protein was purified from bacterial lysates using a nickel–nitrilotriacetic acid agarose matrix according to the manufacturer's instructions (Qiagen, Valencia, CA), which was confirmed to be 35 kDa (His-H1) by anti-H1 Western blot analysis. The eluted protein was dialyzed into PBS plus 500 mM NaCl and flash frozen (Murray, 1991; Maresca *et al.*, 2005).

Xenopus egg extracts

Crude *Xenopus* egg extracts were prepared as described (Murray, 1991; Maresca *et al.*, 2005) and released from metaphase arrest with the addition of 0.5 mM calcium. Cyclohexamide at 50 μg/ml was added to prevent entry into metaphase. The crude extract was further centrifuged at 55,000 rpm (TLS-55 rotor; Beckman Coulter, Fullerton, CA) for 2 h at 4°C. The middle cytoplasmic layer was extracted using an 18-gauge needle and 1-ml syringe and was centrifuged again at 55,000 rpm for 30 min at 4°C to remove residual membranes (Yan *et al.*, 2007). Crude extracts were used for sperm nuclei experiments and high-speed cytoplasm for single-molecule studies. Immunodepletion of >95% histone H1 from extracts or mock (IgG) depletion was performed, using rabbit anti-H1 antibody or IgG antibody, and confirmed by Western blot as described (Maresca *et al.*, 2005). The extracts were immediately aliquoted, flash frozen in liquid nitrogen, and stored at −80°C. To inhibit microtubule assembly, nocodazole was added to crude extracts at a final concentration of 10 ng/μl. The 1-μl samples of extract reactions supplemented with rhodamine tubulin were overlaid with spindle fix and a coverslip as described (Hannak and Heald, 2006), and nuclei were scored manually for stretched or fragmented morphology. For length quantification, random fields of Hoechst-stained nuclei were imaged on an upright epifluorescence microscope (Nikon E600; Nikon, Melville, NY) using a 40× dry objective (numerical aperture, 0.75; Olympus, Tokyo, Japan). Individual nuclei were measured from these images in ImageJ software (National Institutes of Health, Bethesda, MD) by drawing a free-form line lengthwise from the tail proximal to the aster to the distal tip, including any comet-like tail extensions.

Single-DNA tethering

The 48.5-kb λ DNA molecules were end labeled with biotin and digoxigenin as described (Xiao *et al.*, 2010). A ~10-kb supercoilable DNA made by attaching ~900–base pair biotinylated and digoxigeninated DNA segments to a 9.5-kb segment of plasmid pRJ2421 was provided by Reid Johnson (UCLA, Los Angeles, CA). The multiple biotin and digoxigenin at each end of the handles allow it to be supercoilable in stretching experiments (Adams *et al.*, 2006; Taneja *et al.*, 2007). DNAs were bound to paramagnetic microspheres in PBS buffer and mounted onto the flow cell. After single-DNA calibration, the PBS was replaced with XB buffer (100 mM KCl, 1 mM $MgCl_2$, 0.1 mM $CaCl_2$, 10 mM K–4-(2-hydroxyethyl)-1-piperazineethanesulfonic acid [HEPES], pH 7.7, 50 mM sucrose) or XB + KCl buffer (200 mM KCl plus other ingredients).

Single-molecule experiments with extracts

Frozen extract was diluted 1:20 or 1:4 into XB buffer. In dH1+H1 experiments, 1.5 μM recombinant H1 protein was added to the extract before dilution. For every 100 μl of diluted extract, 5 μl of "energy mix" (20 mM MgATP, 200 mM creatine phosphate, and 1 mg/ml creatine kinase in water) was added to obtain a final ATP concentration of 1 mM. Extract was equilibrated at 25°C for 10 min before replacement of the buffer in the sample cell.

Bulk nucleosomal assembly experiments with extracts

Chromatin assembly activity was tested using micrococcal nuclease (MNase) digestion analysis as described (Bonte and Becker, 1999). Chromatin assembly reactions were performed in 55,000 × *g* extract supernatants diluted 1:20 or 1:4 with HEPES buffer (with or without energy mix). In either case, supercoiled pUC18 plasmid was added at a concentration of 2.5 ng/μl and nucleosome (180 base pairs) and dinucleosome (360 base pairs) bands were identified as described (Pope *et al.*, 2002; Wagner *et al.*, 2005). To examine supercoiling, extracts were diluted from 1:10 to 1:100 to assemble DNAs into chromatin fibers. The fibers were treated with proteinase to eliminate the proteins, which resulted in different sizes of supercoiled DNAs. The supercoiled DNAs were further electrophoresed through an agarose gel as described (Tremethick *et al.*, 1990).

ACKNOWLEDGMENTS

We thank Morten Christensen, Hongxia Fu, and Jie Yan for technical assistance and helpful discussions and Meghan McLean and Reid Johnson for providing the pRJ2421 DNA. Work in the Marko lab was supported by the National Science Foundation (DMR-0715099, PHY-0852130, DMR-0520513, MCB-1022117, DMR-1206868), the National Institutes of Health (U54CA143869-01 [NU-PS-OC]), and the Chicago Biomedical Consortium with support from the Searle Funds at the Chicago Community Trust. Work in the Heald lab was supported by the National Institutes of Health (GM057839).

REFERENCES

Adams CD, Schnurr B, Skoko D, Marko JF, Reznikoff WS (2006). Tn5 transposase loops DNA in the absence of Tn5 transposon end sequences. Mol Microbiol 62, 1558–1568.

Al-Natour Z, Hassan AH (2007). Effect of salt on the binding of the linker histone H1 to DNA and nucleosomes. DNA Cell Biol 26, 445–452.

Bennink ML, Leuba SH, Leno GH, Zlatanova J, de Grooth BG, Greve J (2001). Unfolding individual nucleosomes by stretching single chromatin fibers with optical tweezers. Nat Struct Biol 8, 606–610.

Bonte E, Becker PB (1999). Preparation of chromatin assembly extracts from preblastoderm *Drosophila* embryos. Methods Mol Biol 119, 187–194.

Brown DT (2003). Histone H1 and the dynamic regulation of chromatin function. Biochem Cell Biol 81, 221–227.

Clark DJ, Thomas JO (1986). Salt-dependent co-operative interaction of histone H1 with linear DNA. J Mol Biol 187, 569–580.

Dasso M, Dimitrov S, Wolffe AP (1994). Nuclear assembly is independent of linker histones. Proc Natl Acad Sci USA 91, 12477–12481.

Fan Y, Nikitina T, Zhao J, Fleury TJ, Bhattacharyya R, Bouhassira EE, Stein A, Woodcock CL, Skoultchi AI (2005). Histone H1 depletion in mammals alters global chromatin structure but causes specific changes in gene regulation. Cell 123, 1199–1212.

Freedman BS, Heald R (2010). Functional comparison of H1 histones in *Xenopus* reveals isoform-specific regulation by Cdk1 and RanGTP. Curr Biol 20, 1048–1052.

Freedman BS, Miller KE, Heald R (2010). *Xenopus* egg extracts increase dynamics of histone H1 on sperm chromatin. PLoS One 5, e13111.

Fu H, Freedman BS, Lim CT, Heald R, Yan J (2011). Atomic force microscope imaging of chromatin assembled in *Xenopus laevis* egg extract. Chromosoma 120, 245–254.

Graham JS, Johnson RC, Marko JF (2011). Concentration-dependent exchange accelerates turnover of proteins bound to double-stranded DNA. Nucleic Acids Res 39, 2249–2259.

Hannak E, Heald R (2006). Investigating mitotic spindle assembly and function in vitro using *Xenopus laevis* egg extracts. Nat Protoc 1, 2305–2314.
Happel N, Doenecke D (2009). Histone H1 and its isoforms: contribution to chromatin structure and function. Gene 431, 1–12.
Kaplan N *et al*. (2009). The DNA-encoded nucleosome organization of a eukaryotic genome. Nature 458, 362–366.
Kruithof M, Chien FT, Routh A, Logie C, Rhodes D, van Noort J (2009). Single-molecule force spectroscopy reveals a highly compliant helical folding for the 30-nm chromatin fiber. Nat Struct Mol Biol 16, 534–540.
Maresca TJ, Freedman BS, Heald R (2005). Histone H1 is essential for mitotic chromosome architecture and segregation in *Xenopus laevis* egg extracts. J Cell Biol 169, 859–869.
Murray AW (1991). Cell cycle extracts. Methods Cell Biol 36, 581–605.
Pope LH, Bennink ML, Greve J (2002). Optical tweezers stretching of chromatin. J Muscle Res Cell Motil 23, 397–407.
Pope LH, Bennink ML, van Leijenhorst-Groener KA, Nikova D, Greve J, Marko JF (2005). Single chromatin fiber stretching reveals physically distinct populations of disassembly events. Biophys J 88, 3572–3583.
Ramakrishnan V, Finch JT, Graziano V, Lee PL, Sweet RM (1993). Crystal structure of globular domain of histone H5 and its implications for nucleosome binding. Nature 362, 219–223.
Recouvreux P, Lavelle C, Barbi M, Conde ESN, Le Cam E, Victor JM, Viovy JL (2011). Linker histones incorporation maintains chromatin fiber plasticity. Biophys J 100, 2726–2735.
Richardson RT, Batova IN, Widgren EE, Zheng LX, Whitfield M, Marzluff WF, O'Rand MG (2000). Characterization of the histone H1-binding protein, NASP, as a cell cycle-regulated somatic protein. J Biol Chem 275, 30378–30386.
Rosidi B, Wang M, Wu W, Sharma A, Wang H, Iliakis G (2008). Histone H1 functions as a stimulatory factor in backup pathways of NHEJ. Nucleic Acids Res 36, 1610–1623.
Ruberti I, Worcel A (1986). Mechanism of chromatin assembly in *Xenopus* oocytes. J Mol Biol 189, 457–476.
Skoko D, Wong B, Johnson RC, Marko JF (2004). Micromechanical analysis of the binding of DNA-bending proteins HMGB1, NHP6A, and HU reveals their ability to form highly stable DNA-protein complexes. Biochemistry 43, 13867–13874.
Skoko D, Yan J, Johnson RC, Marko JF (2005). Low-force DNA condensation and discontinuous high-force decondensation reveal a loop-stabilizing function of the protein Fis. Phys Rev Lett 95, 208101.
Skoko D, Yoo D, Bai H, Schnurr B, Yan J, McLeod SM, Marko JF, Johnson RC (2006). Mechanism of chromosome compaction and looping by the *Escherichia coli* nucleoid protein Fis. J Mol Biol 364, 777–798.
Smith RC, Dworkin-Rastl E, Dworkin MB (1988). Expression of a histone H1-like protein is restricted to early *Xenopus* development. Genes Dev 2, 1284–1295.
Syed SH, Goutte-Gattat D, Becker N, Meyer S, Shukla MS, Hayes JJ, Everaers R, Angelov D, Bednar J, Dimitrov S (2010). Single-base resolution mapping of H1-nucleosome interactions and 3D organization of the nucleosome. Proc Natl Acad Sci USA 107, 9620–9625.
Taneja B, Schnurr B, Slesarev A, Marko JF, Mondragon A (2007). Topoisomerase V relaxes supercoiled DNA by a constrained swiveling mechanism. Proc Natl Acad Sci USA 104, 14670–14675.
Thastrom A, Gottesfeld JM, Luger K, Widom J (2004). Histone-DNA binding free energy cannot be measured in dilution-driven dissociation experiments. Biochemistry 43, 736–741.
Thoma F, Koller T, Klug A (1979). Involvement of histone H1 in the organization of the nucleosome and of the salt-dependent superstructures of chromatin. J Cell Biol 83, 403–427.
Thomas JO, Rees C, Finch JT (1992). Cooperative binding of the globular domains of histones H1 and H5 to DNA. Nucleic Acids Res 20, 187–194.
Tremethick D, Zucker K, Worcel A (1990). The transcription complex of the 5 S RNA gene, but not transcription factor IIIA alone, prevents nucleosomal repression of transcription. J Biol Chem 265, 5014–5023.
Ura K, Nightingale K, Wolffe AP (1996). Differential association of HMG1 and linker histones B4 and H1 with dinucleosomal DNA: structural transitions and transcriptional repression. EMBO J 15, 4959–4969.
van Holde K, Zlatanova J (1996). What determines the folding of the chromatin fiber? Proc Natl Acad Sci USA 93, 10548–10555.
Wagner G, Bancaud A, Quivy JP, Clapier C, Almouzni G, Viovy JL (2005). Compaction kinetics on single DNAs: purified nucleosome reconstitution systems versus crude extract. Biophys J 89, 3647–3659.
Weischet WO, Allen JR, Riedel G, Van Holde KE (1979). The effects of salt concentration and H-1 depletion on the digestion of calf thymus chromatin by micrococcal nuclease. Nucleic Acids Res 6, 1843–1862.
Xiao B, Johnson RC, Marko JF (2010). Modulation of HU-DNA interactions by salt concentration and applied force. Nucleic Acids Res 38, 6176–6185.
Xiao B, Zhang H, Johnson RC, Marko JF (2011). Force-driven unbinding of proteins HU and Fis from DNA quantified using a thermodynamic Maxwell relation. Nucleic Acids Res 39, 5568–5577.
Yan J, Maresca TJ, Skoko D, Adams CD, Xiao B, Christensen MO, Heald R, Marko JF (2007). Micromanipulation studies of chromatin fibers in *Xenopus* egg extracts reveal ATP-dependent chromatin assembly dynamics. Mol Biol Cell 18, 464–474.

Supplementary Data

Histone H1 compacts DNA under force and during chromatin assembly

Botao Xiao, Benjamin S. Freedman, Kelly E. Miller, Rebecca Heald, and John F. Marko

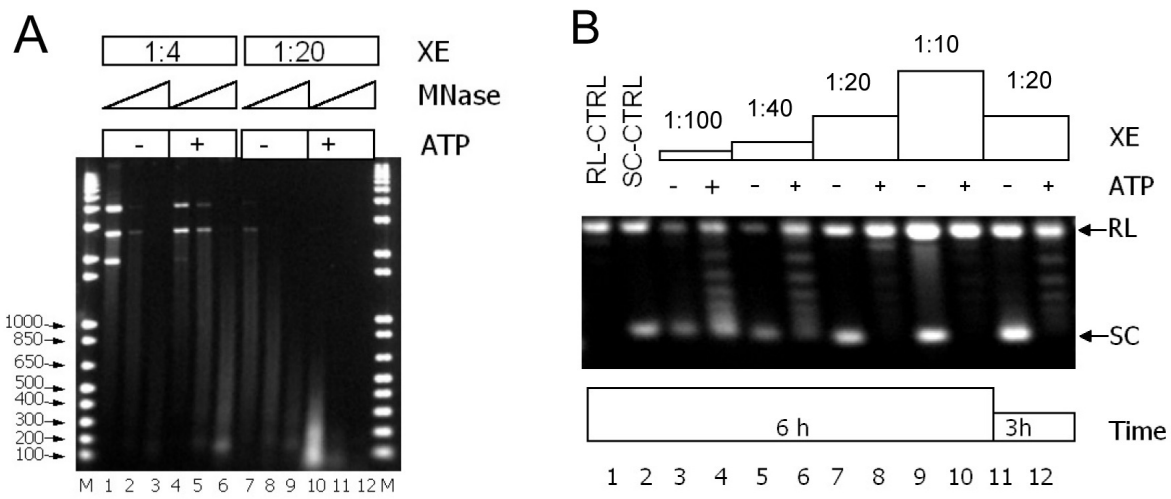

Figure S1.

Results of bulk nucleosome assembly experiments.

A. MNase digestions assay. 180 and 360 bp segments were found in ATP-containing chromatin assembly reactions in *Xenopus* extracts (XE), diluted either 1:4 or 1:20.

B. DNA supercoiling assay. Relaxed (RL) and supercoiled (SC) DNAs (2.7 kb) were used as control. The DNAs were incubated with XE for 3 and 6 hours in different samples. Supercoiled DNA segments of different sizes were observed in the presence of ATP.

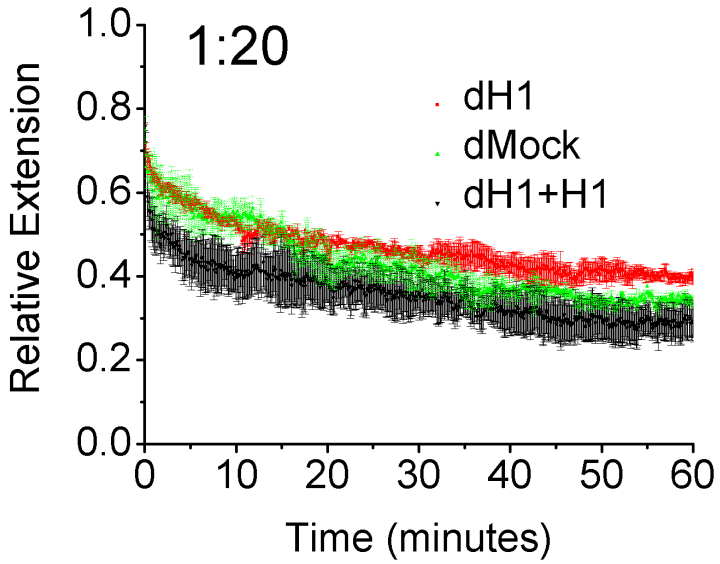

Figure S2.

DNA compaction in dMock, dH1, and dH1+H1, diluted 20 times (1:20). The data are smoothed and labeled with standard error (S.E.M.). The force was held at 0.7 pN. After 60 minutes of assembly, the average relative extension of dH1 was (40 ± 1)%, longer than dMock (34% ± 1%, p = 0.0265) and dH1+H1 (29% ± 4%, p = 0.048).

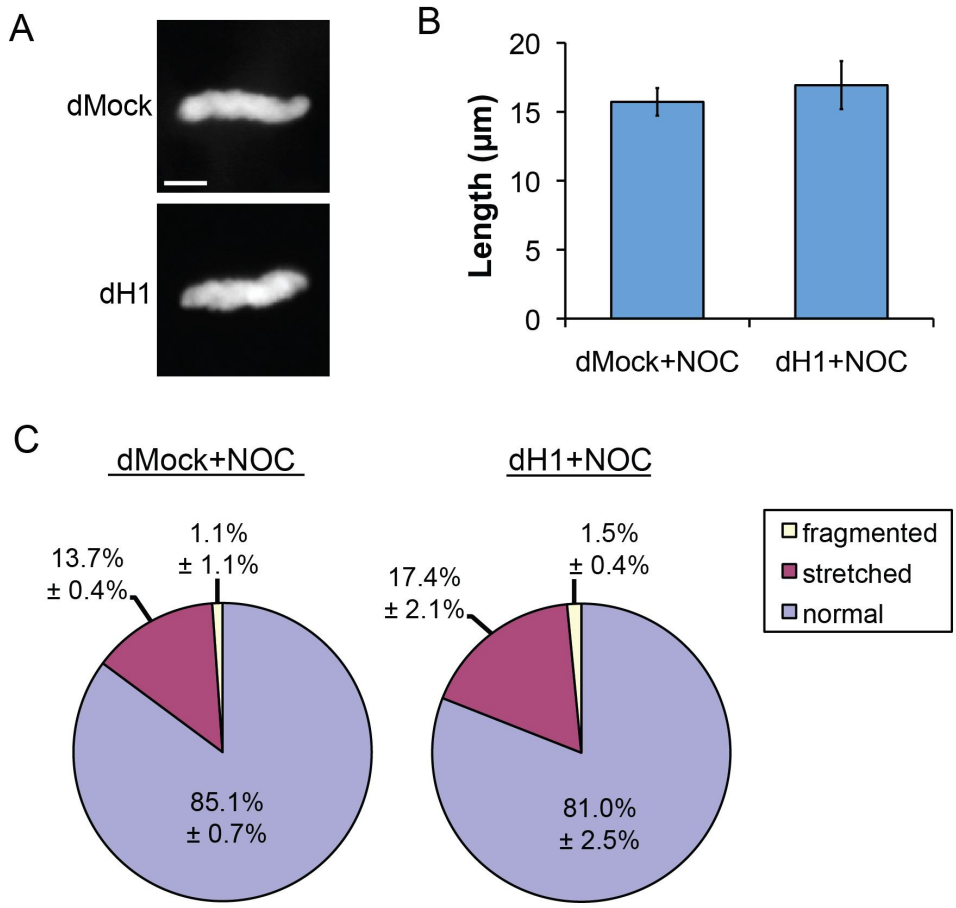

Figure S3

Effect of H1 on sperm nuclei in the presence of nocodazole.

A. Representative images of sperm nuclear DNA (DAPI) in dMock or dH1 egg extracts treated with 10 ng/µl nocodazole (NOC). Scale bar, 5 µm.

B. Measurement of sperm nuclear lengths from tail-to-tip ten minutes after addition of sperm nuclei. Mean sperm lengths were determined in separate experiments (~25 nuclei per experiment, n = 4 experiments) and averaged.

C. Quantification of normal, stretched, and fragmented nuclei in nocodazole-treated reactions. Error bars, standard error.